Applied Surface Science 255 (2009) 8629–8633

Contents lists available at ScienceDirect

Applied Surface Science

journal homepage: www.elsevier.com/locate/apsusc

# Influence of annealing temperature on microstructure and optical properties of sol–gel derived tungsten oxide films

Xilian Sun *, Hongtao Cao, Zhimin Liu, Jianzhong Li

*Division of Functional Materials and Nano Devices, Ningbo Institute of Material of Technology & Engineering, Chinese Academy Sciences, Ningbo 315203, PR China*

ARTICLE INFO

*Article history:*
Received 27 December 2008
Received in revised form 30 April 2009
Accepted 9 June 2009
Available online 17 June 2009

*PACS:*
42.70–a
81.07–b

*Keywords:*
Electrochromic thin films
Tungstic oxide
Microstructure
Optical properties

ABSTRACT

Tungsten oxide ($WO_3$) thin films have been extensively studied for their interesting physical properties and a variety of potential applications in electrochromic devices. In order to explore the possibility of using these in electrochromic devices, a preliminary and thorough study of the optical properties of the host materials is an important step. Based on this, the influence of annealing temperature on the structural, surface morphological, optical and electrochromic properties has been investigated in the present work. The host material, $WO_3$ films, has been prepared from an ethanolic acetylated peroxotungstic acid sol containing 5 wt.% oxalic acid dehydrate (OAD) by sol–gel technique. The monoclinic structure and textured nature change of the films with the temperature increasing have been investigated by X-ray diffraction analysis. The surface morphology evolution of the films has been characterized by SEM. The shift in absorption edge towards the higher wavelength region observed from optical studies may be due to the electron scattering effects and the optical band filling effect that reveals the crystallization of the film. The amorphous film shows better optical modulation ($\Delta T = 76.9\%$ at $\lambda = 610$ nm), fast color-bleach kinetics ($t_c \sim 4$ s and $t_b \sim 9$ s) and good reversibility ($Q_b/Q_c = 90\%$), thereby rendering it suitable for smart window applications.



## 1. Introduction

Electrochromic thin films are of much interest in contemporary and emerging technology, where they can be used for regulating the throughput of radiant energy in "smart windows", the luminous reflectance in "antidazzling" mirrors, the contrast in nonemissive information displays, and the thermal emittance in temperature control devices [1]. Tungsten oxide ($WO_3$) has been extensively studied and is reported to have interesting physical properties, which makes it suitable for above electrochromic applications [2]. And almost all oxide-based EC devices employ tungsten oxide [3]. The electrochromic properties of amorphous $WO_3$ thin films have been investigated extensively because it is a superior inorganic electrochromic material with regard to coloration efficiency and cyclic durability [4–9]. This instigated us to restrict ourselves towards evaluating the potential of highly disordered thin films of $WO_3$ for smart window applications. The $WO_3$ film is quite porous and smaller alkali ions can be easily intercalated and deintercalated into it. The density of the films starts to increase significantly upon a post annealing temperature of 250 °C [10]. Moreover, the electrochromic performance of $WO_3$ films basically depends on their structural, surface morphological, compositional and optical properties. It is important that the improvement of materials' properties requires a closer inspection of preparation conditions. Various techniques, such as vacuum evaporation [11], chemical vapor deposition [12], sputtering [13], spray deposition [9], sol–gel processing [14–18], etc. have been utilized for deposition of $WO_3$ films. Out of which the sol–gel processing being cost-effective, has good control over the microstructrue and homogeneity of the coatings [19]. Therefore, this technique has also been used for the development of electrochromic coating with the materials, either tungsten alkoxides $W(OR)_6$ or tungsten oxyalkoxide $WO(OR)_4$ or $WO_2(OR)_2$. But these precursors are not stable towards hydrolysis or condensation. Hence the peroxo route has been considered largely for the growth of $WO_3$ films. In this route, oxalic acid dehydrate (OAD) as a chelating agent is often applied to tailor the microstructure and grain size of the $WO_3$ films and hence the optical and electrochromic properties of the films have been improved [17]. The effect of microstructure modification brought about by doping with varying OAD content on the transmission and reflection modulation, optical absorption coefficient and band gap, switching kinetics, electrochemical activity and the charge storage properties of $\alpha$-$WO_3$ films have been evaluated [10]. But the volume of data concerning the structural and optical evolution of the films as a function of annealing temperature falls off rapidly. The present study focuses on the annealing temperature on the structural, morphological and optical properties of $WO_3$ films in a

* Corresponding author. Tel.: +86 574 86685163; fax: +86 574 86685163.
*E-mail address:* xiliansun@163.com (X. Sun).

0169-4332/$ – see front matter © 2009 Elsevier B.V. All rights reserved.
doi:10.1016/j.apsusc.2009.06.042

detailed manner and attempts to provide valuable insights into the electrochromic properties of the $WO_3$ films.

## 2. Experimental

### 2.1. Tungsten oxide film deposition

The tungsten oxide thin films used in this study were prepared by the sol–gel route combined with spin-coating method. 13 g of tungsten metal powder at 99.9% purity were slowly added to a mixture of 80 ml of 30% $H_2O_2$ and 8 ml of deionized water yielding a colorless solution of peroxotungstic acid. The reaction being exothermic was conducted at 5 °C. The clear solution obtained upon filtration was refluxed at 55 °C for 24 h after addition of 80 ml of glacial acetic acid. The resulting pale yellow solution was vacuum dried at 60 °C to obtain a yellow flaky solid of acetylated peroxotungstic acid. The solid material (20 g) was dissolved in 60 ml of ethanol by heating at ~50 °C and to the resulting clear and bright yellow solution, 5 wt.% of oxalic acid dehydrate (OAD) (with respect to the weight of the sol) was added in. The sol was spin-coated onto transparent conducting substrates ($SnO_2$:F coated glass of $1 \times 1\ cm^2$ dimensions, 14 Ω/sq) at 3500 rpm for 30 s. Before deposition, the FTO-covered glasses were ultrasonically cleaned in both acetone and ethanol followed by rinsing with distilled water. The samples were dried at 60 °C for 2 min after deposition. To achieve the desired film thickness, the samples were spin-coated three times followed by heat treatment. All films were annealed from room temperature to 100 °C at the rate of 5 °C/min in air and held at this temperature for 1 h and then brought back to room temperature. Finally, they were heated to 250 °C, 350 °C, 450 °C at the same heating rate respectively and held at this temperature for 3 h and gradually cooled to room temperature.

### 2.2. Characterization techniques

Film thickness and refractive index measurements were performed with a Woollam M-2000 spectroscopic ellipsometer at λ = 546.1 nm, using incidence angles of 50°, 60° and 70°. X-ray diffraction (XRD) patterns of the virgin films were recorded in the $2\theta$ range from 10° to 70° with a Bruker AXS D8 advance diffractometer, using Cu Kα (λ = 1.5406 Å) radiation. A scanning electron microscope (SEM, S-4800, Hitachi) was used for studying the surface morphological characteristics. Transmittance (T) spectra for virgin, colored and bleached $WO_3$ films, were recorded ex situ in the 300–2000 nm wavelength range with respect to air in the reference beam in a Lambda 950 UV-Vis-NIR spectrophotometer (PerkinElmer). Switching time characteristics between the colored and bleached states for $WO_3$ films were recorded by double chronoamperometry with a square wave potential of ±1 V for activating the electrochromic electrode in an electrolyte solution of lithium perchlorate in propylene carbonate (1 M $LiClO_4$-PC). Cyclic voltammetry for the film was performed in a classical three-electrode electrochemical cell between −1 V and +1 V with a scan rate of 20 mV/s wherein a $WO_3$ film deposited on a $SnO_2$:F coated glass substrate acted as the working electrode, Ag/AgCl/KCl was employed as the reference electrode and a Pt rod was used as the auxiliary electrode. The measurements were performed in a liquid electrolyte (1 M $LiClO_4$-PC).

## 3. Results and discussions

### 3.1. X-ray diffraction analysis

X-ray diffraction patterns of the $WO_3$ films annealed at 250 °C, 350 °C and 450 °C are shown in Fig. 1(a–c). The amorphous nature of $WO_3$ films has been observed in the pattern (Fig. 1(a)) for film annealed at 250 °C. When the films have been subjected to the higher annealing treatment at $T_{anneal}$ = 350 °C (Fig. 1(b)), the formation of triplet peaks has been observed. For the post heat treated films at 450 °C, the XRD pattern (Fig. 1(c)) shows high intensity and well oriented with the enhancement of crystalline quality. The observed structural parameters were compared with JCPDS (no. 83-0950) data and they are in good agreement with the monoclinic crystalline structure. Also the formation of triplet peaks along (0 0 *l*), (0 *k* 0) and (*h* 0 0) growth orientations (where *h* = *k* = *l* = 2) shows that the films are grown along 'c', 'b', 'a' axes respectively confirming the columnar and textured growth nature of the films.

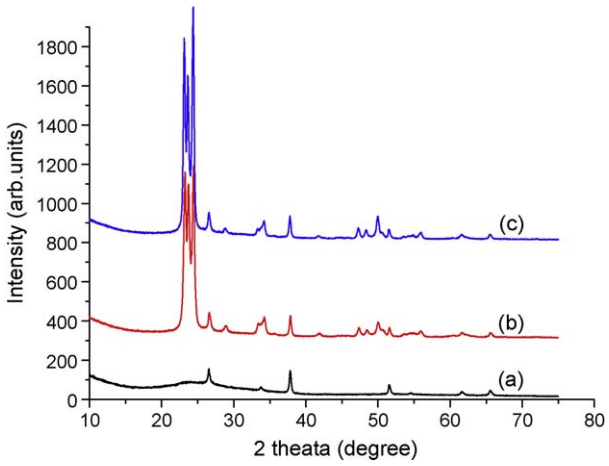


**Fig. 1.** X-ray diffractogram of $WO_3$ films annealed at different temperatures: (a) 250 °C, (b) 350 °C and (c) 450 °C. The stars (*) indicate $SnO_2$.

The average grain sizes of $WO_3$ films annealed at 350 °C and 450 °C were calculated by using the Scherrer's formula and is about 19.9 nm and 28.6 nm, respectively, which confirmed the nano-crystalline nature of the films. It shows that crystallite size of the films is increased with increasing annealing temperature. The intense sharp peaks in X-ray diffraction pattern reveal the good crystallinity of the films and also confirm the stoichiometric nature of $WO_3$ films. The single phase nature of the films was also confirmed from the presence of XRD peaks pertaining only to the $WO_3$ phase. With the increasing annealing temperatures the intensity of the diffracted peaks becomes more intense and sharp. The enhanced preferential orientation after annealing at high temperatures may be due to the movement of atoms along the surface of the substrate to reach the low energy nucleation sites and growing preferentially there itself.

### 3.2. Scanning electron microscopic analysis

The surface morphological features of the as-prepared and annealed film are presented in Fig. 2. The image of the film annealed at 250 °C reveals the uniform amorphous surface nature. When the films were annealed at 350 °C (Fig. 2(b)), the morphology becomes a netted surface. As the annealing temperature increases to 450 °C, an entirely different surface morphology (Fig. 2(c)) is obtained. The surface looks like well resolved and crystallized with uniform needle-like textured grain morphology. This indicates the crystalline nature of the films subjected to a post heat treatment at 450 °C. These needle-like crystallites confirm the highly textured nature as evident from the prominently observed triplet peaks along (0 0 2), (0 2 0) and (2 0 0) orientations (Fig. 2(c)).

It is clearly observed from the surface morphological studies by scanning electron microscope that all the films have surfaces with uniform, homogenous and spherical grain morphology. Cracks

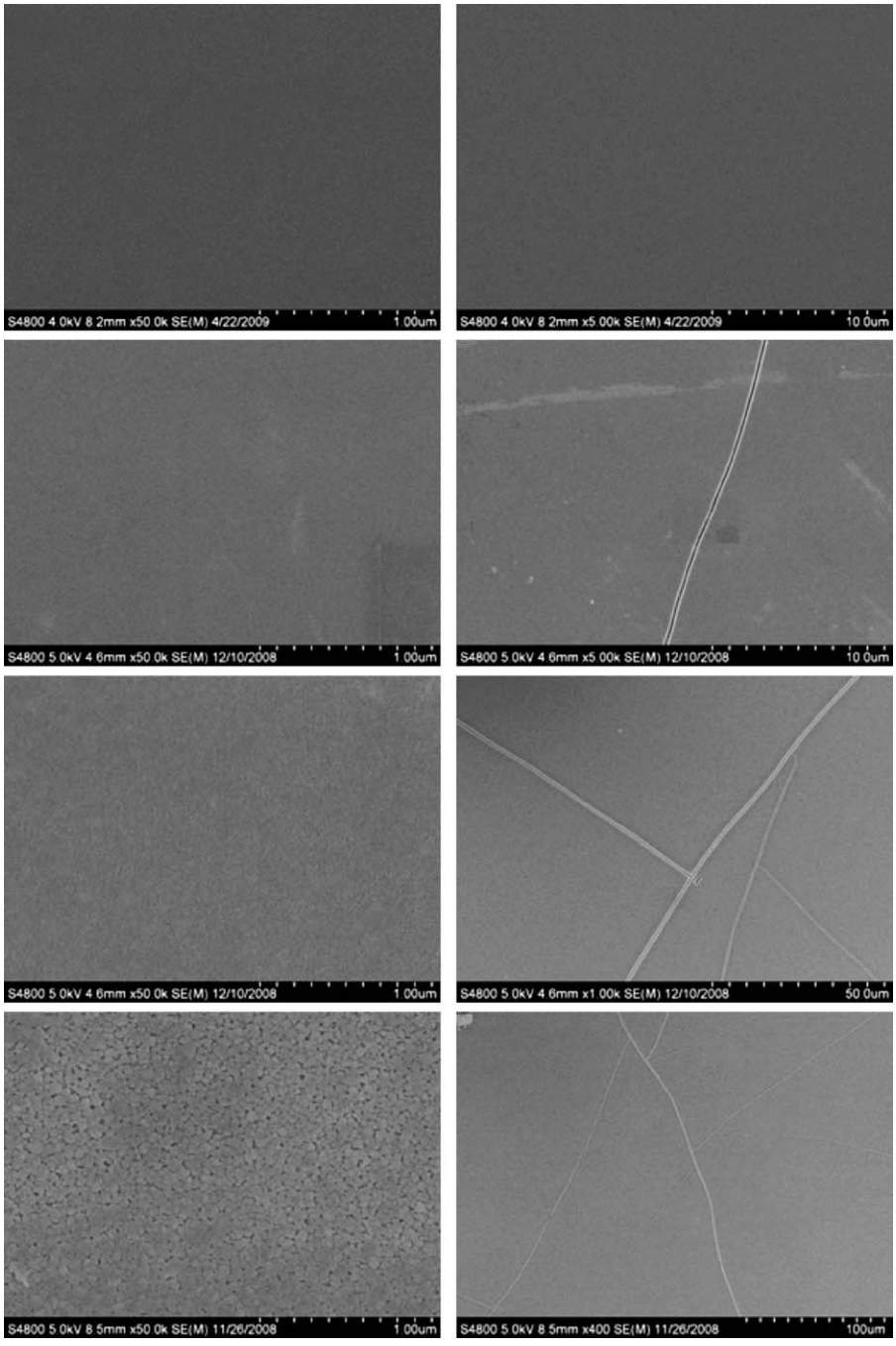


**Fig. 2.** SEM micrographs of as-prepared and annealed $WO_3$ films at (a) 250 °C, (b) 350 °C and (c) 450 °C.

exist on the annealed film texture which is due to the strain imposed on the layer during the heat treatment and the removal of the water (dehydration). Our study revealed that these cracks do not affect the electrochromic properties of the films.

### 3.3. Optical and electrochemical properties

The variation in refractive index and thickness of the film as a function of annealing temperature are listed in Table 1. The film thickness is 333 nm, 263 nm and 255 nm for films annealed at 250 °C, 350 °C and 450 °C, respectively. The refractive indices of tungsten oxide increase with annealing temperature increase, indicating an increase in film density. Fig. 3(a) and (b) illustrates the optical transmittance and absorptance spectra of the virgin, colored and bleached nanostructured $WO_3$ films annealed at different temperatures in the wavelength range 300–2000 nm. It is obvious that the maximum transmittance for the virgin films annealed at 250 °C are about 77% ($\lambda$ = 510 nm), with a variation of 62–77% in the visible region but declines rapidly beyond 1200 nm (Fig. 3(a)). At 350 °C and 450 °C, the heat effects lead to the

**Table 1**
Film thickness and refractive index of the $WO_3$ films annealed at different temperatures.

| Annealing temperature (°C) | Film thickness, $d$ (nm) | Refractive index, $n$ ($\lambda$ = 546 nm) |
|---|---|---|
| 250 | 333 | 1.79 |
| 350 | 263 | 1.92 |
| 450 | 255 | 1.96 |

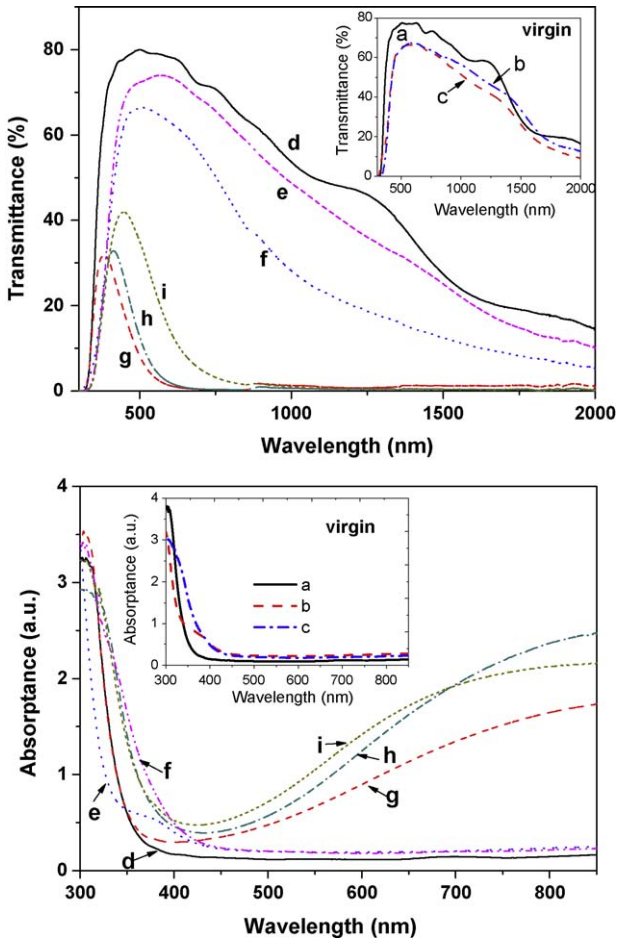


**Fig. 3.** (a) Transmittance and (b) absorptance spectra of virgin (a,b,c), bleached (d,e,f) and colored (g,h,i) $WO_3$ films annealed at 250 °C (a,d,g), 350 °C (b,e,h) and 450 °C (c,f,i).

densification of $WO_3$, drastically reducing the transparency. It is also observed from the transmittance spectra that the absorption edge is also slightly shifted towards the longer wavelength region for the films annealed at higher temperatures which is seen in the absorptance spectrum (Fig. 3(b)), owing to preferred colored effect on the films. The result is consistent with those of other authors who have reported that the absorption peak moves to lower energy caused by a disappearance of short W=O bonds for the crystalline

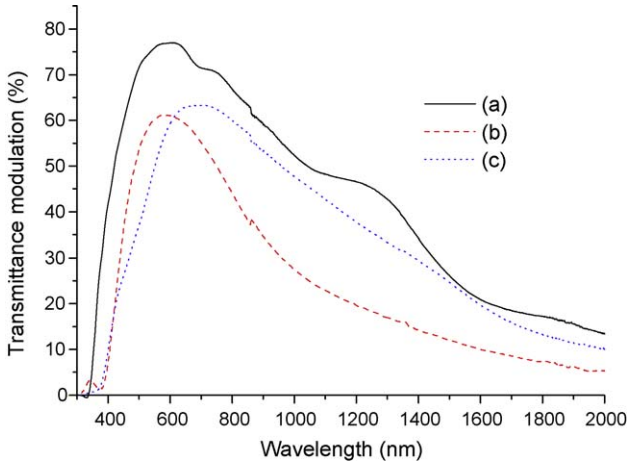


**Fig. 4.** Transmittance modulation ($\Delta T$) of $WO_3$ films annealed at (a) 250 °C, (b) 350 °C and (c) 450 °C.

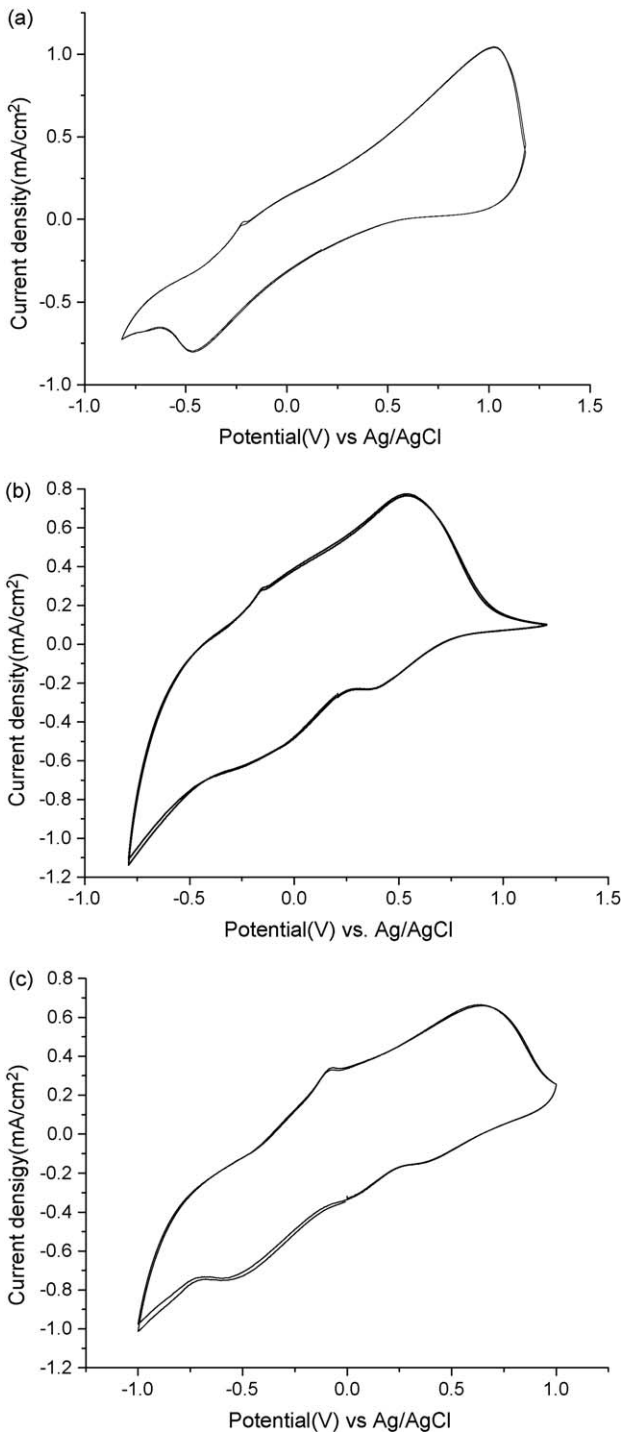


**Fig. 5.** Cyclic voltammograms for $WO_3$ films annealed at (a) 250 °C, (b) 350 °C and (c) 450 °C recorded at a scan speed of 20 mV/s in a 1 M $LiClO_4$-PC electrolyte.

structures [20]. The transmission modulation ($\Delta T$) of the films annealed at 250 °C varies between 41% and 76% in the visible range and drops abruptly in the near-infrared (*NIR*) wavelengths (Fig. 4). This $\Delta T$ drop could be attributed to an increased absorptance and reflectance at *NIR* wavelengths in the colored states. With the annealing temperature increasing to 350 °C and 450 °C, the maximum $\Delta T$ drops to 60%. This indicates that amorphous films exhibit the largest modulation of visible radiation, whereas crystalline films show a dominant attenuation of radiation.

**Table 2**
Coloration-bleaching times and charge storage capacity of $WO_3$ films annealed at different temperatures.

| Annealing temperature (°C) | Coloration time (s) | Bleaching time, $t_c$ (s) | Ion storage capacity (mC $m^{-2}$) |
|---|---|---|---|
| 250 | 4 | 9 | 60 |
| 350 | 10 | >300 | 50 |
| 450 | 20 | >300 | 46 |

In Fig. 3(b), for the absorptance spectrum of colored films, a low absorption region that looks like a valley in the spectrum is observed around 450 nm, this is the cause of the blue coloration of tungsten oxide. It is also seen that the spectra for all the colored films show a high absorption region at longer wavelengths. And the absorption increases with the annealing temperature increasing, which may be due to the electron scattering effects and the optical band filling effect that reveals the crystallization of the film.

Typical cyclic voltammograms recorded at a scan speed of 20 mV/s for all films under investigation are displayed in Fig. 5. The reversibility during the electrochemical reactions can be estimated by the ratio of the charge densities ($Q_a/Q_c$): 0.90, 0.68 and 0.66 for the films annealing at 250 °C, 350 °C and 450 °C, respectively. It is apparent that the electrochemical reversibility of films annealed at 250 °C exceeds that of the films annealed at 350 °C and 450 °C. About 90% of the inserted charge could be extracted in the following oxidation step while the insertion reversibility drops to 68% and 66% with the annealing temperature increasing to 350 °C and 450 °C, respectively. The low value of the insertion reversibility indicated trapping of the $Li^+$ ions in the framework, probably due to the densification structure and small pore of the crystalline towards Li insertion. It is also seen that the voltammogram profiles corresponding to the film annealed at 250 °C is different from the other annealed films and the reported CV plots in Ref. [17], which may be due to the different microstructure, including film density and surface roughness. The average roughness of all annealed films is 3.37 nm, 4.19 nm and 5.9 nm, respectively, which were higher than that of $WO_3$ films from Ref. [17]. This different microstructure brings about changes in the RC equivalent circuit and different shapes of the voltammograms [21].

The films were also colored using a two-step potential of −1 V to +1 V yielding the current flowing through the working electrode as a function of time in order to determine the response times and ion storage capacities of the film. In this report, the coloration time $t_c$ and the bleaching time $t_b$ is defined as the time required for the cathodic/anodic current of the film to attain a steady state in the coloration/bleaching cycle, after application of respective voltages. The coloring/bleaching kinetic data for the three samples are compared in Table 2. To avoid an initial cycling effect, six coloration-bleaching cycles were performed on all samples before the real data-gathering experiment commenced. It has been found that coloration kinetics is observed to be faster than bleaching kinetics for all the films. Annealing temperature does influence coloring and bleaching kinetics. It is evident that the microstructure of films annealed at 250 °C is most favorable for a rapid ion intercalation and deintercalation process as these films exhibit faster coloring-bleaching kinetics and higher charge storage capacity than the films annealed at higher temperatures.

## 4. Conclusion

This study has shown the effect of annealing temperature on structural, surface morphological, optical and electrochromic properties of tungsten oxide ($WO_3$) films formed from a sol–gel derived precursor sol of acetylated peroxotungstic acid with 5wt.% oxalic acid dehydrate. X-ray diffraction analysis clearly shows the formation of predominant triplet peaks along (0 0 2), (0 2 0) and (2 0 0) growth orientations, which exhibits the monoclinic, single phase and textured growth nature of the films annealed at 350 °C and 450 °C. The transformation of amorphous to polycrystalline nature of the films was observed when we increase the annealing temperature. The better aligned and highly oriented growth peaks enumerate the stoichiometric nature of the films. The nanostructural nature of $WO_3$ films prepared at different annealing temperatures are evident from the surface morphological results reported here. Higher annealing temperature enhances the growth of oriented nanocrystalline thin films and decreases the transmittance. The transmittance modulation in the visible range is higher for the film annealed at 250 °C and decreases at higher annealing temperature. The shift in absorption edge towards longer wavelength region has been assigned to the coloration effect of the films. The insertion reversibility is 90% for films annealed at 250 °C and decreases to 68% and 66% for higher annealing temperature. The present data could help to develop general strategies for the improvement of electrochromic devices based on $WO_3$.

## Acknowledgments

This study was financially supported by Science and Technology Department of Zhejiang Province of China (2008C31G3220006). The authors acknowledge the help of Prof. Hongtao Cao and Dr. Jianzhong Li for performing the electrochemical measurements.

## References

[1] A. Azens, A. Hjelm, D. Le Bellac, C.G. Granqvist, SPIE 2351 (1995) 92.
[2] D. Manno, A. Serra, M.Di. Guilio, G. Micocci, A. Tepore, Thin Solid Films 324 (1998) 44.
[3] G.A. Niklasson, C.G. Granqvist, J. Mater. Chem. 17 (2007) 127.
[4] C.G. Granqvist, Handbook of Inorganic Electrochromic Materials, Elsevier, Amsterdam, 1995.
[5] C.G. Granqvist, Sol. Energy Mater. Sol. Cells 60 (2000) 201.
[6] C.M. Lampert, Sol. Energy Mater. Sol. Cells 76 (2003) 489.
[7] E. Avendano, L. Bergren, G.A. Niklasson, C.G. Granqvist, A. Azens, Thin Solid Films 496 (2006) 30.
[8] K. Nakagawa, N. Miura, S. Matsumoto, R. Nakano, H. Matsumoto, Jpn. J. Appl. Phys. 47 (2008) 7230.
[9] S.R. Bathe, P.S. Patil, Solid State Ionics 179 (2008) 314.
[10] N. Sharma, M. Deepa, P. Varshney, S.A. Agnihotry, Thin Solid Films 401 (2001) 45.
[11] J. Garcia-Canadas, F. Fabregat-Santiago, I. Porqueras, et al. Solid State Ionics 175 (2004) 521.
[12] T. Ivanova, K.A. Gesheva, G. Popkirov, M. Ganchev, E. Tzvetkova, Mater. Sci. Eng. B 119 (2005) 232.
[13] H. Sadiki, J.F. Pierson, C. Rousselot, N. Martin, G. Terwagne, Surf. Coat. Technol. 200 (2005) 232.
[14] M. Deepa, A.K. Srivastava, M. Kar, S.A. Agnihotry, J. Phys. D: Appl. Phys. 39 (2006) 1885.
[15] A.E. Aliev, H.W. Shin, Solid State Ionics 154–155 (2002) 425.
[16] M. Deepa, A.K. Srivastava, K.N. Sood, S.A. Agnihotry, Nanotechnology 17 (2006) 2625.
[17] M. Deepa, R. Sharma, A. Basu, S.A. Agnihotry, Electrochim. Acta 50 (2005) 3545.
[18] K. Huang, J.F. Jia, Q.T. Pan, F. Yang, D.Y. He, Physica B 396 (2007) 164.
[19] P.K. Biswas, N.C. Pramanik, M.K. Mahapatra, D. Ganguli, J. Livage, Mater. Lett. 57 (2003) 4429.
[20] J.J. Kleperis, P.D. Chikmach, A.R. Lusis, Phys. Status Solidi A 83 (1984) 291.
[21] J.G. Canadas, I.M. Sero, F.F. Santiago, J. Bisquert, G.G. Belmonte, J. Electroanal. Chem. 565 (2004) 329.